Cellular Dynamics international
a FUJIFILM company

Apply Today to Receive Free Cells

Jumpstart your new project with ready-to-use iPSC-derived cells! CDI is awarding a limited number of *free* vials of differentiated cells for innovative research. Choose from any of our neuroscience-related products. To apply:*

www.cellulardynamics.com/grants

* Conditions and restrictions may apply.

STEM CELLS®

REGENERATIVE MEDICINE

Epidermal Growth Factor and Granulocyte Colony Stimulating Factor Signaling Are Synergistic for Hematopoietic Regeneration

SADHNA O. PIRYANI,[a] ANGEL Y. F. KAM,[a] EVELYNA G. KLIASSOV,[a] BENNY J. CHEN,[a,b] NEIL L. SPECTOR,[b,c] JOHN P. CHUTE,[d,e,f] DAVID S. HSU,[b,c] NELSON J. CHAO,[a,b] PHUONG L. DOAN [a,b]

Key Words. Hematopoietic regeneration • Epidermal growth factor • Granulocyte colony stimulating factor • Chemotherapy • Hematopoietic stem cells (HSCs)

[a]Division of Hematologic Malignancies and Cellular Therapy, [b]Duke Cancer Institute, and [c]Division of Medical Oncology, Duke University, Durham, North Carolina, USA; [d]Division of Medical Oncology, [e]Eli and Edythe Broad Center for Regenerative Medicine and Stem Cell Research, and [f]Jonsson Comprehensive Cancer Center, University of California, Los Angeles, Los Angeles, California, USA

Correspondence: Phuong L. Doan, M.D., 595 LaSalle Street, DUMC 103866, Durham, North Carolina 27710, USA. Telephone: 919-613-2625; e-mail: Phuong.Doan@duke.edu

Received August 5, 2017; accepted for publication October 24, 2017; first published online in STEM CELLS *EXPRESS* October 31, 2017.

http://dx.doi.org/10.1002/stem.2731

ABSTRACT

Hematopoietic regeneration following chemotherapy may be distinct from regeneration following radiation. While we have shown that epidermal growth factor (EGF) accelerates regeneration following radiation, its role following chemotherapy is currently unknown. We sought to identify EGF as a hematopoietic growth factor for chemotherapy-induced myelosuppression. Following 5-fluorouracil (5-FU), EGF accelerated hematopoietic stem cell regeneration and prolonged survival compared with saline-treated mice. To mitigate chemotherapy-induced injury to endothelial cells in vivo, we deleted *Bax* in VEcadherin^{+} cells (*VEcadherinCre;Bax*$^{FL/FL}$ mice). Following 5-FU, *VEcadherinCre;Bax*$^{FL/FL}$ mice displayed preserved hematopoietic stem/progenitor content compared with littermate controls. 5-FU and EGF treatment resulted in increased cellular proliferation, decreased apoptosis, and increased DNA double-strand break repair by non-homologous end-joining recombination compared with saline-treated control mice. When granulocyte colony stimulating factor (G-CSF) is given with EGF, this combination was synergistic for regeneration compared with either G-CSF or EGF alone. EGF increased G-CSF receptor (G-CSFR) expression following 5-FU. Conversely, G-CSF treatment increased both EGF receptor (EGFR) and phosphorylation of EGFR in hematopoietic stem/progenitor cells. In humans, the expression of EGFR is increased in patients with colorectal cancer treated with 5-FU compared with cancer patients not on 5-FU. Similarly, EGFR signaling is responsive to G-CSF in humans in vivo with both increased EGFR and phospho-EGFR in healthy human donors following G-CSF treatment compared with donors who did not receive G-CSF. These data identify EGF as a hematopoietic growth factor following myelosuppressive chemotherapy and that dual therapy with EGF and G-CSF may be an effective method to accelerate hematopoietic regeneration. STEM CELLS *2017; 00:000–000*

SIGNIFICANCE STATEMENT

Whether epidermal growth factor (EGF), like granulocyte colony stimulating factor (G-CSF), promotes hematopoietic regeneration following chemotherapy is unknown. We demonstrate that EGF accelerates hematopoietic regeneration by increasing expression of G-CSF receptor. After 5-fluorouracil, administration of EGF and G-CSF was synergistic compared with either EGF or G-CSF alone. These data indicate that dual therapy with EGF and G-CSF could accelerate hematopoietic recovery following chemotherapy-induced myelosuppression.

INTRODUCTION

Hematopoietic growth factors, like granulocyte colony stimulating factor (G-CSF), have clinical indications for the treatment of cytopenias due to chemotherapy or radiotherapy. To accelerate hematopoietic regeneration, G-CSF has resulted in shortened duration of neutropenia [1–3] by signaling through its receptor, G-CSFR, which is expressed on non-hematopoietic and hematopoietic cells, including hematopoietic stem cells (HSCs) [4].

HSCs reside adjacent to bone marrow (BM) endothelial cells (ECs) [5]. These ECs provide instruction to HSCs in both homeostasis and following myelosuppressive stress [6–10]. Transplantation of ECs can restore hematopoiesis, even following lethal-dose total body

irradiation [11–13]. Even without transplantation of ECs, EC-derived soluble factors are sufficient to expand hematopoietic cells [14–17]. Recently, we described that pharmacologic administration of epidermal growth factor (EGF) resulted in both a 10-fold expansion of HSC-repopulating capacity and survival advantage compared with controls following radiation injury [18]. While EGF may be a radiation mitigator, its role in HSC regeneration following chemotherapy and how EGF compares with G-CSF for treatment of chemo-induced myelosuppression are yet to be determined. These questions are translationally relevant since the mechanisms for hematopoietic injury following radiation can differ from those following chemotherapy injury. For example, differences in patterns of damage to hematopoietic cells exist following 5-fluorouracil (5-FU) compared with radiation [19]. Moreover, the morphology of damaged sinusoidal ECs may be discontinuous and hemorrhagic following ionizing radiation, which differs from ECs observed following 5-FU, where ECs were non-discontinuous and non-hemorrhagic [20]. These differences in the response of both HSCs and ECs to chemotherapy or radiation suggest that there could be differences in the marrow's response to growth factors as well.

The goal of this study is to characterize the hematopoietic response to both myelosuppressive and lethal-dose chemotherapy following EGF. Here, we demonstrate that EGF expanded HSCs and prolonged survival following 5-FU compared with saline-treated mice. Using mice with deletion of *Bax* in VEcadherin-expressing cells, we confirmed the fundamental role of ECs in facilitating hematopoietic regeneration. EGF increased G-CSFR expression, and mutually, G-CSF increased both EGF receptor (EGFR) and phosphorylation of EGFR. Translationally, in humans, 5-FU increases EGFR expression, and G-CSF in healthy human donors increases both EGFR and phosphorylation of EGFR. Taken together, these data demonstrate that EGF and G-CSF are synergistic to promote hematopoietic regeneration and could be given as dual therapy to patients with EGFR-negative malignancies undergoing chemotherapy treatment.

Materials and Methods

Animals and Chemical/Biologic Reagents

Eight to 12-week old C57Bl6 (CD 45.2^+) and B6.SJL (CD 45.1^+) mice were purchased from Jackson Laboratory (Bar Harbor, ME). Biologic variables such as age, sex, and weight were matched. By breeding *VECadherinCre;Bax*$^{FL/+}$ mice with *Bax*$^{FL/FL}$ mice, we generated both *VECadherinCre;Bax*$^{FL/FL}$ mice and *VECadherinCre;Bax*$^{FL/+}$. Duke University Animal Care and Use Committee has approved all animal studies.

5-Fluorouracil (Fresenius Kabi, Lake Zurich, IL) and 5-fluoro-2′-deoxyuridine 5′-monophosphate (FdUMP), an active metabolite of 5-FU (Sigma-Alrich, St. Louis, MO), were diluted with 1X PBS (Sigma-Alrich) to the specified concentrations.

Peripheral blood (PB) samples from both healthy donors and patients with colorectal cancer (CRC) were obtained using protocols approved by the Institutional Review Board at Duke University. Written and informed consents were obtained from all subjects. PB from healthy donors, donors mobilized with G-CSF, and patients with CRC was collected in heparinized tubes. For mobilization, donors were treated with daily injections of 10 μg/kg G-CSF per day for 5 days. Samples were collected and processed 2 hours after the last dose.

Early passage patient-derived cancer cell lines were cultured and developed as described previously [21]. CRC patients' specimens used to generate the cell lines were collected under a Duke IRB approved protocol (Pro00002435). These cell lines were then authenticated using the Duke University DNA Analysis Facility Human cell line authentication (CLA) service. Specifically, genomic DNA isolated from the cancer cell lines were analyzed for polymorphic short tandem repeat markers using the GenePrint 10 kit from Promega (Madison, WI) to ensure purity. HT-29, HCT-116, and NCI-H460 were obtained from American Type Culture Collection (Manassas, VA). Cultures of primary BM ECs were generated using methods described previously [18].

Analysis for EGF, EGFR, and G-CSFR Expression

For mRNA expression of EGFR, cell subsets from C57Bl6 mice were collected at 24 hours following 150 mg/kg 5-FU, 0.5 mg/kg IV EGF (R&D Systems, Minneapolis, MN), or 0.5 mg/kg subcutaneously G-CSF. mRNA EGFR expression analyses and analysis for other targets (CDK1, CDK2, CDK4, CDK6, p21, PUMA, and BCl-2) were performed according to manufacturer's specifications (ThermoFisher Scientific, Waltham, MA). Relative expression of genes was calculated using delta–delta C_T analysis with normalization to *GAPDH*.

For protein expression of EGFR, cell subsets were isolated according to manufacturer's specifications (Miltenyi Biotec, Auburn, CA). BM lineage-negative (lin^-) cells were stained with CD34 APC (BD), anti-EGFR FITC (Abcam, Cambridge, MA), 7-AAD (BD), and anti-lineage antibody APC, anti-cKit PE, and anti-Sca-1 APC-Cy7 (BD, San Jose, CA). Phosphorylation of EGFR was performed using published methods [18].

G-CSFR expression was determined using ckit + Sca + Lin- (KSL) antibodies (BD) and anti-G-CSFR antibody Alexafluor 488 (R&D Systems).

For phospho-EGFR of human cells, cells were labeled with CD34+, and then cells were fixed and permeabilized as described [18]. Cells were labeled with anti-phospho-EGFR (Y1078) antibody (Cell Signaling, Danvers, MA). Isotype controls were included for all analyses.

Hematopoietic Progenitor Cell Assays and Survival Study

BM collection, mouse EC antigen-32 (MECA) staining, and colony forming cell (CFCs) methylcellulose assays were performed using published methods [18]. H&E staining were performed by the Duke Research Immunohistology Laboratory. For colony-forming unit-spleen 12 (CFU-S12) analysis, 2×10^5 whole BM (WBM) cells were injected into 900-cGy irradiated C57Bl6 mice. At day 12 post-injection, colonies were counted by two independent investigators. Complete blood counts were quantified on a HemaVet 950 (Drew Scientific, Dallas, TX). Long-term culture initiating cell (LTC-IC) assays were performed using published methods [22].

Competitive transplantation assays were performed with 2×10^5 donor cells from B6.SJL mice at day 7 after 5-FU and days 1–4 of 0.5 mg/kg EGF or saline and injected into 900-cGy irradiated C57Bl6 mice with 2×10^5 host WBM cells. Secondary competitive transplantation assays were performed using 40% of BM cells from primary-transplanted mice and 2×10^5 host WBM cells. Each donor was transplanted into

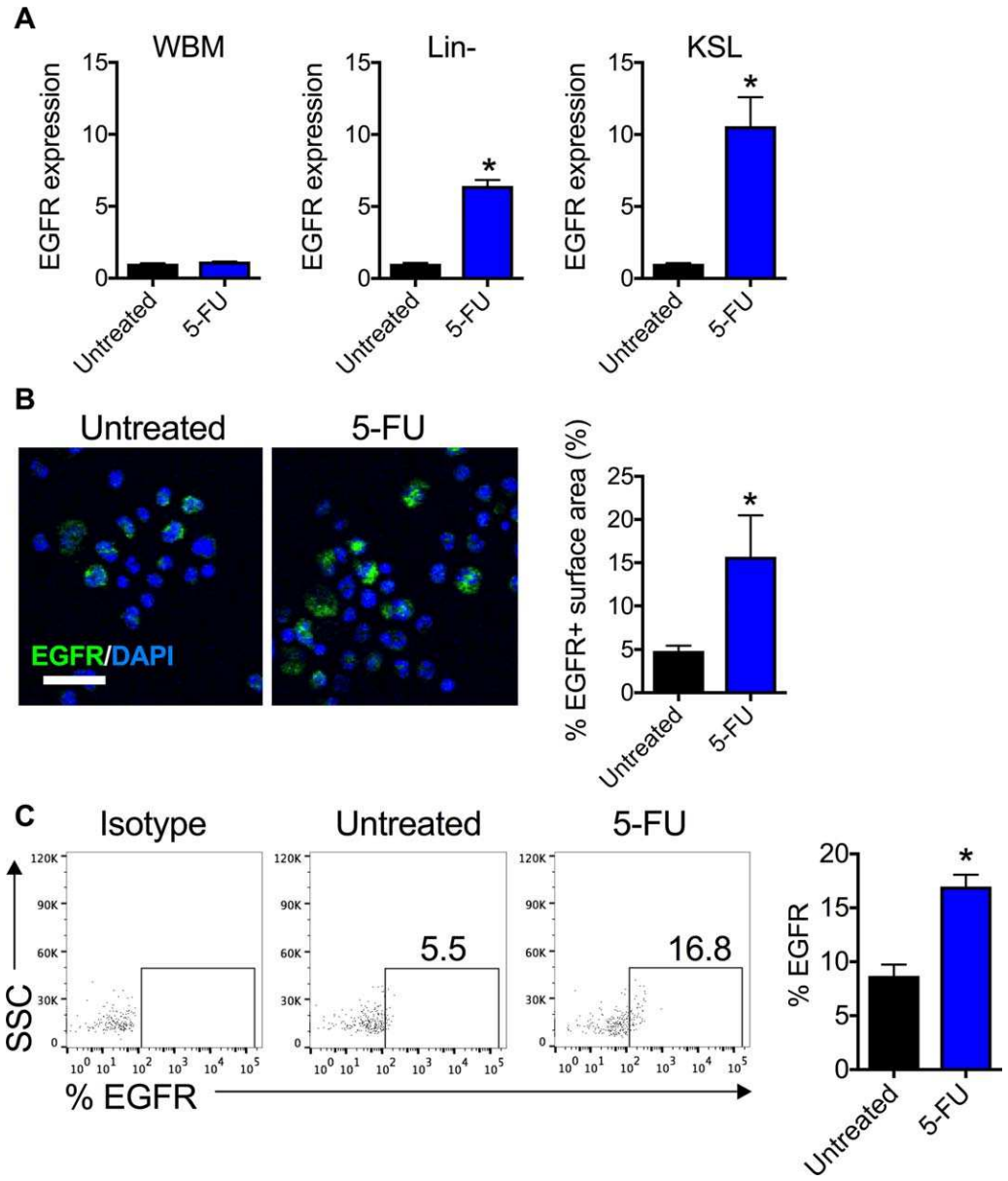

Figure 1. Epidermal growth factor receptor (EGFR) on HSPCs increases following 5-fluorouracil (5-FU). **(A):** EGFR mRNA expression at baseline and 24 hours following 150 mg/kg 5-FU. $n = 3$–12 per group. *, $p < .0001$. **(B):** EGFR (green) in bone marrow (BM) lin$^-$ cells compared with control. DNA is stained with 4′,6-diamidino-2-phenylindole (blue). Scale bar = 25 μm. Percentage BM lin$^-$ EGFR+ pixels normalized by surface area. $n = 8$–9 per group. *, $p = .03$. **(C):** Representative flow cytometric analysis of percentage EGFR in ckit + Sca + Lin- cells from mice at 24 hours following 5-FU compared with untreated mice. Quantification of EGFR expression. $n = 4$–6 per group. *, $p = .0008$. Abbreviations: DAPI, 4′,6-diamidino-2-phenylindole; EGFR, epidermal growth factor receptor; 5-FU, 5-fluorouracil; KSL, ckit + Sca + Lin-; HSPCs, hematopoietic stem and progenitor cells; SSC, side scatter; WBM, whole bone marrow.

two recipient mice. Measurement of donor chimerism within the BM KSL population was performed at 16-weeks post-transplantation as described previously [18].

For the survival study, C57Bl6 mice were treated with 600 mg/kg IV 5-FU and then given 0.5 mg/kg EGF or saline beginning at 24 hours later and then daily through day 4. Mice were sacrificed when endpoints were met according to approved protocols from IACUC at Duke University.

HSC Cycling and Cell Death Assays

For cell cycle analysis, KSL-labeled cells were treated with Fix Buffer I, Perm Buffer III, Ki67-FITC, and 7-AAD according to manufacturer specifications (BD). For cell death analysis, KSL cells were sorted and cultured for 24 hours in 0.5 μM FdUMP with and without 20 ng/ml EGF in 20 ng/ml thrombopoietin, 125 ng/ml stem cell factor, and 50 ng/ml Flt-3 ligand (TSF) [18] compared with TSF alone. KSL cells and progeny were stained with annexin V FITC and 7-AAD according to manufacturer's specifications (BD).

Viability of cells were determined by tetrazolium blue (MTT, Sigma-Alrich) assay according to manufacturer's specifications.

Statistical Analyses and Image Capture

Data are shown as means ± SEM. Student's *t* test (two-tailed with unequal variance) or Mann-Whitney analysis were used

as specified in the figure legends. Survival analysis was performed using a Log-rank test. Analyses were performed using GraphPad Prism (v7.0, La Jolla, CA).

Images for immunohistochemistical analysis were obtained with Zeiss AxioImager Z2 and Axiocam 506. Immunofluorescent images were obtained with an Olympus BX61WI two photon system (Center Valley, PA). Adobe Photoshop software (20142.2, Adobe Systems, San Jose, CA) was used to quantify positive signals using methods previously described [23].

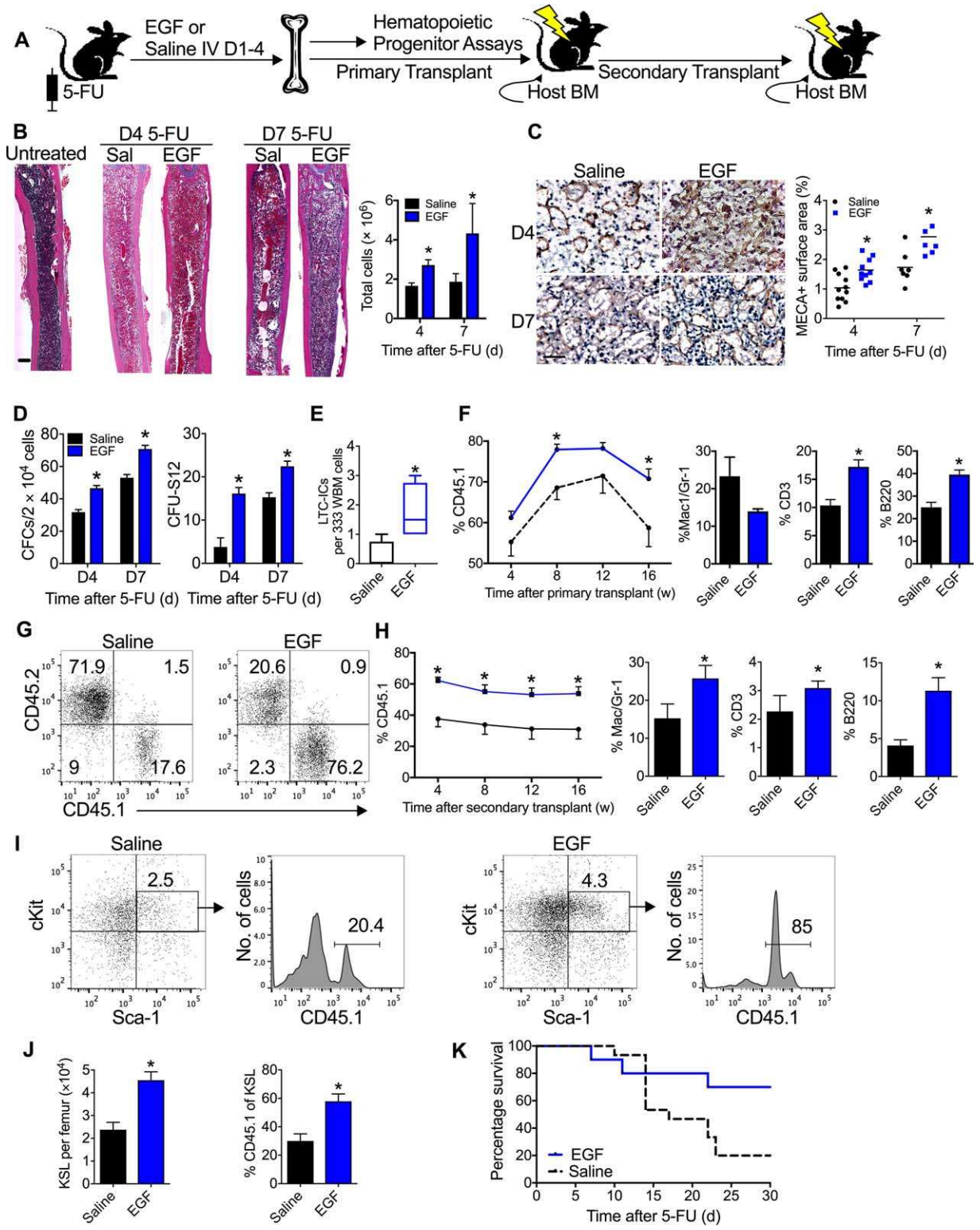

Figure 2.

Results

EGFR Expression Is Induced Following 5-FU

Following radiation, EGFR expression is enriched in KSL cells compared with more differentiated progenitor cells [18]. Untreated animals displayed increased EGFR expression in KSL cells compared with lin$^-$ cells (Supporting Information Fig. S1A). At 24 hours following 5-FU, KSL cells have a 10.5-fold increase in EGFR mRNA expression compared with untreated animals (Fig. 1A). Comparison of EGFR expression in KSL cells with lin$^-$ cells following 5-FU treatment demonstrate increased EGFR expression, indicating that 5-FU enriches EGFR-expressing cell within the KSL subset (Supporting Information Fig. S1A). EGFR immunofluorescence in BM lin$^-$ cells displayed a 3.2-fold increase in EGFR compared with untreated mice (Fig. 1B). Flow cytometric analysis for EGFR in both the WBM and lin$^-$ cell populations displayed less than 2% of EGFR+ cells in either untreated or 5-FU-treated animals. The percentage of EGFR+ cells within the KSL subset was increased 24.4-fold compared with WBM from untreated mice (Fig. 1C). Comparison of the total KSL cells that are EGFR+ in untreated and 5-FU-treated mice show a modest increase in EGFR expression (Supporting Information Fig. S1B). Taken together, following 5-FU, both mRNA and protein expression of EGFR is increased in hematopoietic cells, and particularly in KSL cells.

EGF Promotes HSC Reconstitution Following 5-FU

To determine whether EGF accelerates HSC reconstitution after 5-FU, C57Bl6 mice were treated with 5-FU and then EGF or saline starting 24 hours later, since growth factors like G-CSF are administered at 24 hours following chemotherapy (Fig. 2A). BM was analyzed on both day 4 and day 7, since with 5-FU, day 4 represents the hematopoietic nadir and regeneration has commenced by day 7 [19]. At these time points, EGF-treated mice displayed preserved BM cellularity with a 2.3-fold increase in total cells at day 7 in EGF-treated animals compared with saline-treated mice (Fig. 2B). The marrow vasculature also demonstrated increased staining for ECs by MECA (Fig. 2C). EGF-treated mice increased CFCs and CFU-S12 compared with saline-treated mice (Fig. 2B–2D). LTC-IC assays, which are in vitro assays that linearly correlate with HSC function in vivo [24, 25], demonstrated a 7-fold increase in long-term HSCs in EGF-treated mice compared with saline-treated mice (Fig. 2E).

Complementary to LTC-IC assays, we performed competitive transplantation assays. Primary donor engraftment in both the PB and marrow of recipients of WBM from EGF-treated animals had increased multi-lineage donor engraftment compared with recipients of saline-treated animals (Fig. 2F). Secondary competitive transplants were performed in which BM from primary recipient mice was transplanted into lethally irradiated recipients with competing host WBM. As early as 4 weeks and throughout the period of monitoring until 16 weeks, recipients of EGF-treated donor cell had increased PB engraftment compared with recipients of saline-treated donor cells (Fig. 2G, 2H). Moreover, recipients of EGF-treated donors had both increased CD 45.1 chimerism and total KSL cells (Fig. 2I, 2J). These results indicate that pharmacologic treatment of EGF accelerated hematopoietic regeneration following myelosuppressive-dose 5-FU, particularly within the stem cell pool.

EGF Prolongs Survival Following Lethal-Dose 5-FU

To determine whether EGF prolongs survival following lethal-dose 5-FU injury, C57Bl6 mice were treated with 600 mg/kg 5-FU and then EGF or saline from days 1 to 4 (Fig. 2K). Seventy percent of EGF-treated animals (7 of 10) survived through day 30. In contrast, only 20% of saline-treated animals (3 of 15) survived until day 30. These results demonstrate that EGF provides a survival advantage following lethal-dose chemotherapy.

Deletion of *Bax* in VEcadherin+ ECs Is Chemoprotective of HSPCs

At 24 hours following 5-FU, the expression of *Bax*, a pro-apoptotic gene, is increased 2.8-fold in BM lin$^-$ cells from mice treated with 5-FU compared with untreated mice (Fig. 3A). To abrogate apoptotic cell death in ECs, we used *CreLoxP*

Figure 2. Pharmacologic treatment of epidermal growth factor (EGF) accelerates hematopoietic stem cell reconstitution following 5-fluorouracil (5-FU). **(A):** C57Bl6 or B6.SJL mice were treated with 150 mg/kg IV 5-FU, then 0.5 mg/kg EGF or saline on days 1–4. Hematopoietic assays were performed on days 4 and 7. **(B):** Left, femurs stained with H&E. Scale bar = 500 μm (left) and 100 μm (right). Right, total cells per femur from saline- (black) or EGF-treated mice (blue). n = 18–22 per group for day 4. n = 7–9 per group for day 7. *, p = .002 and .04 by Mann-Whitney analysis for days 4 and 7, respectively. **(C):** Left, femurs at days 4 and 7 following 5-FU chemotherapy and treatment with EGF or saline. Representative sections of mouse endothelial cell antigen-32 (MECA)- (brown) and hematoxylin (blue)-stained femurs. Scale bar = 100 μm. Right, quantification of percentage of MECA+ pixels per surface area at days 4 and 7. n = 10–11 per group for day 4, *, p = .005. n = 7 per group; *, p = .008 for day 7. **(D):** Left, colony forming cells, n = 9–15 per group. *, $p < .0001$ for days 4 and 7. Right, colony-forming unit-spleen 12, n = 5–7 per group. *, p = .0005 and *, p = .0007 for days 4 and 7, respectively. **(E):** Six-week long-term culture initiating cells. n = 4 per group. *, p = .03. **(F):** Peripheral blood (PB) CD45.1+ engraftment from EGF-treated mice (blue) compared with saline-treated control mice (black) at day 7 following 5-FU. Recipients received 2×10^5 whole bone marrow (WBM) donor cells and 2×10^5 competing host WBM. n = 8–10 per group; *, p = .009 and .03 for 8 and 16 weeks, respectively. Percentage myeloid (Mac1/Gr-1), T-cell (CD3), and B-cell (B220) engraftment at 16 weeks in the PB of recipient mice. *, p = .0009 for %CD3 and *, p = .0005 for % B220 by Mann-Whitney analysis. **(G):** Representative flow cytometric analysis at 16-weeks post-secondary transplantation of total donor cell engraftment in marrow of recipient mice. **(H):** PB donor cell engraftment following secondary transplantation at 16-week after primary transplantation of 40% of WBM cells from 5-FU and EGF- or saline-treated donor mice and 2×10^5 WBM host cells. n = 11–17 per group. *, p = .0001; .01; .01; and .007 for 4, 8, 12, and 16 weeks, respectively by Mann-Whitney analysis. Percentage myeloid, T-, and B-cell engraftment at 16 weeks in the bone marrow (BM) of recipient mice. *, p = .009; .006; .0008, respectively by Mann-Whitney analysis. **(I):** Flow cytometric analysis from a live, lin$^-$ gate of total donor engraftment in BM ckit + Sca + Lin- (KSL) cells at 16 weeks. **(J):** KSL cells per femur and percentage donor CD 45.1 cells within the KSL population are shown. *, p = .0003 and .001, respectively. **(K):** Survival following 600 mg/kg IV 5-FU and EGF or saline. n = 10–15 per group. *, p = .04 by Log-rank analysis. Abbreviations: BM, bone marrow; CFC, colony forming cell; CFU-S12, colony-forming unit-spleen 12; EGF, epidermal growth factor; 5-FU, 5-fluorouracil; KSL, ckit + Sca + Lin-; LTC-IC, long-term culture initiating cell; MECA, mouse endothelial cell antigen-32; WBM, whole bone marrow.

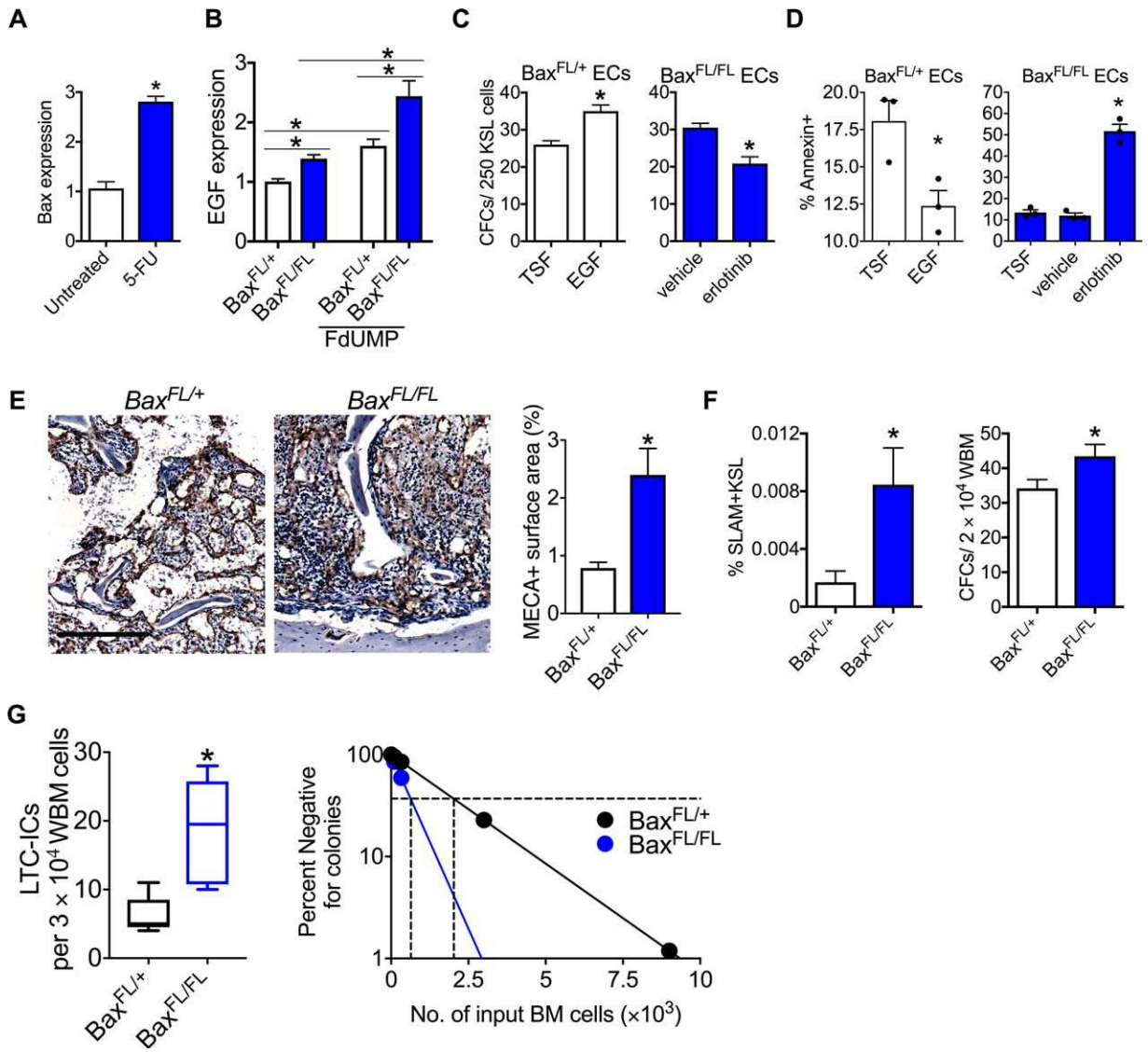

Figure 3. Deletion of *Bax* in VEcadherin+ endothelial cells (ECs) abrogates HSPC injury. **(A):** *Bax* mRNA expression in bone marrow (BM) lin$^-$ cells at 24 hours after 5-fluorouracil (5-FU). $n = 8$ per group. *, $p < .0001$. **(B):** Epidermal growth factor (EGF) mRNA expression in $Bax^{FL/+}$ and $Bax^{FL/FL}$ ECs at steady state and following 24 hours in culture with 0.5 μM 5-fluoro-2′-deoxyuridine 5′-monophosphate (FdUMP). $n = 6$ per group. *. $p = .007$ for $Bax^{FL/+}$ and $Bax^{FL/FL}$ ECs at steady state; *, $p = .01$ for $Bax^{FL/+}$ and $Bax^{FL/FL}$ ECs with FdUMP. *, $p = .005$ for $Bax^{FL/+}$ ECs following FdUMP treatment. *, $p = .003$ for $Bax^{FL/FL}$ ECs following FdUMP treatment. **(C):** Colony forming cells (CFCs) and **(D):** % annexin+ cells at 48 hours from non-contact cultures of C57Bl6 ckit + Sca + Lin- (KSL) cells with $Bax^{FL/+}$ ECs and EGF or TSF alone (white bars) or $Bax^{FL/FL}$ ECs and erlotinib or vehicle (blue bars). $n = 6$ per group. *, $p = .001$. $n = 3$ per group for % annexin+. *, $p = .03$ and .0003 for $Bax^{FL/+}$ and $Bax^{FL/FL}$ conditions, respectively. **(E):** Left, mouse endothelial cell antigen-32 (MECA)-stained femurs from $Bax^{FL/+}$ and $Bax^{FL/FL}$ mice on day 4 following 5-FU. Scale bar = 250 μm. Right, quantification of percentage MECA+ pixels. $n = 7$–8 per group. *, $p = .007$. **(F):** Percentage SLAM$^+$KSL cells and CFCs of $Bax^{FL/+}$ and $Bax^{FL/FL}$ mice on day 4 after 5-FU. $n = 4$–12 per group. *, $p = .03$ and .04, respectively. **(G):** Six-week long-term culture initiating cells (LTC-ICs) on day 4 following 5-FU. $n = 5$–6 per group. *, $p = .007$. Poisson statistical analysis of a limiting dilution assay of 6-week LTC-ICs from $Bax^{FL/+}$ and $Bax^{FL/FL}$ BM cells following 5-FU on day 4. The LTC-IC frequency of $Bax^{FL/FL}$ mice was 1 in 636 compared with 1 in 2,030 cells for $Bax^{FL/+}$ mice. $n = 5$–6 per cell dose per group. Abbreviations: BM, bone marrow; CFC, colony forming cell; EC, endothelial cell; EGF, epidermal growth factor; fdUMP, 5-fluoro-2′-deoxyuridine 5′-monophosphate; 5-FU, 5-fluorouracil; HSPC, hematopoietic stem and progenitor cell; KSL, ckit + Sca + Lin-; LTC-IC, long-term culture initiating cell; MECA, mouse endothelial cell antigen-32; TSF, thrombopoietin, stem cell factor, and FMS-like tyrosine kinase 3 ligand.

technology to delete *Bax* in VECadherin$^+$ ECs in *VECadherin-Cre;*$Bax^{FL/FL}$ ($Bax^{FL/FL}$) mice and littermate control *VECadherin-Cre;*$Bax^{FL/+}$ ($Bax^{FL/+}$) mice, which retained one *Bax* allele (Supporting Information Fig. S2A). Without injury to these mice, we detected no differences in complete blood counts, BM cellularity, BM EC structure or density, SLAM$^+$KSL cells, or CFCs (Supporting Information Fig. S2B–S2F).

We sought to determine whether prevention of chemotherapy-induced apoptotic cell death within VEcadherin$^+$ ECs would result in accelerated HSPC reconstitution. Following 24-hour cultures of BM lin$^-$ cells from each genotype with TSF + FdUMP or TSF alone, no differences were noted in total cell expansion, %KSL, and CFCs, suggesting that the hematopoietic phenotypes are equal (Supporting Information Fig. S2G). The

phenotype of ECs, however, differ in that ECs from $Bax^{FL/FL}$ mice displayed increased levels of EGF compared with ECs from $Bax^{FL/+}$ mice both at baseline and at 24 hours following culture with FdUMP (Fig. 3B). FdUMP increased EGF expression in cultured ECs from both genotypes. This increase in EGF expression was greater in $Bax^{FL/FL}$ ECs compared with $Bax^{FL/+}$ ECs (Fig. 3B). Non-contact cultures of C57Bl6 KSL cells and FdUMP with $Bax^{FL/+}$ ECs and TSF + EGF displayed increased CFCs and decreased annexin+ cells compared with cultures with $Bax^{FL/+}$ ECs and TSF alone (Fig. 3C, 3D). Conversely, non-contact cultures of C57Bl6 KSL cells and FdUMP with $Bax^{FL/FL}$ ECs and erlotinib, an inhibitor for EGFR [26], resulted in decreased CFCs and a 4.3-fold increase in annexin+

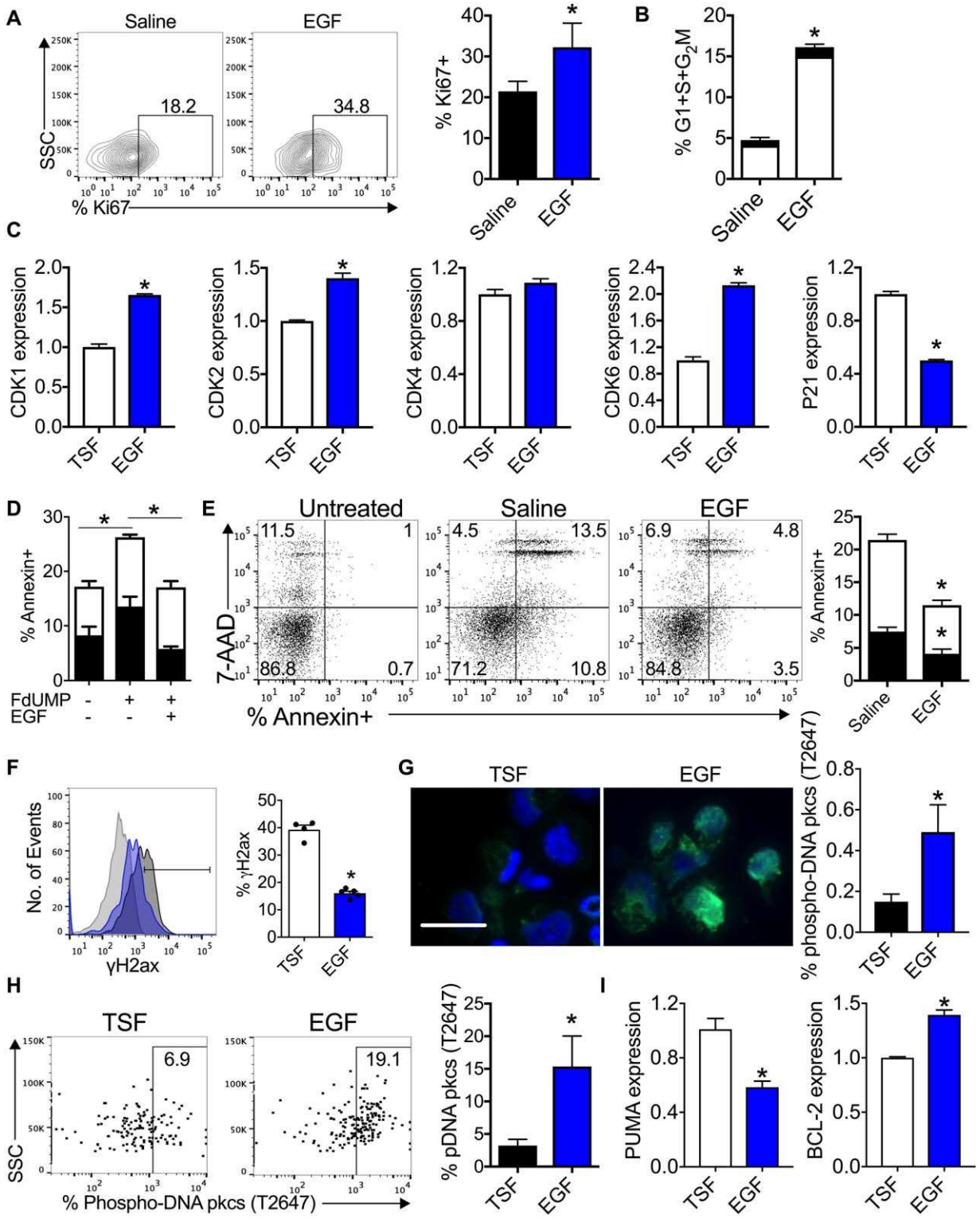

Figure 4.

cells. Following 5-FU, $Bax^{FL/FL}$ mice display increased marrow and vascular content, increased $SLAM^+$KSL cells, and CFCs compared with $Bax^{FL/+}$ mice (Fig. 3E, 3F). More specifically, $Bax^{FL/FL}$ mice had a 3.1-fold increase in MECA+ cells in their marrow compared with $Bax^{FL/+}$ mice (Fig. 3E). Similarly, total HSC content of $Bax^{FL/FL}$ mice was threefold greater compared with $Bax^{FL/+}$ mice as estimated by LTC-IC assays (Fig. 3G). These data demonstrate that *Bax* deficiency in VEcadherin-expressing cells could abrogate the myelosuppressive impact of 5-FU on HSCs in vivo. These data demonstrate that increased levels of EGF in vivo results in accelerated HSC regeneration following 5-FU myelosuppression.

Mechanisms of EGF Activity in HSPCs

We sought to determine whether EGF signaling could promote hematopoietic cell proliferation following chemotherapy. On day 4 following 5-FU, EGF-treated mice displayed increased Ki67+ cells compared with saline-treated mice (Fig. 4A). This increased level of Ki67 cells corresponded to increased KSL cells that were cycling in interphase (Fig. 4B). Since cyclin-dependent kinases (CDKs) tightly regulate cell cycle [27], we showed that EGF could upregulate CDK expression (CDK1, CDK2, and CDK6) and downregulate the CDK inhibitor p21 following chemotherapy (Fig. 4C).

Since EGF mediated cell proliferation, we sought to determine whether EGF signaling could also mitigate chemo-induced cellular apoptosis. With the addition of EGF to KSL cell cultures treated with FdUMP, annexin+ cells were diminished compared with cultures with TSF alone (Fig. 4D). In vivo, C57Bl6 mice treated with 5-FU and EGF displayed a 54% decrease in annexin+ cells compared with saline-treated control mice (Fig. 4E).

Since 5-FU exerts its cytotoxic effects in part by generating lethal double-strand DNA (dsDNA) breaks [28], we hypothesized that the decrease in annexin+ cells following EGF was by enhanced DNA repair [29]. Following 24 hours culture with FdUMP, EGF-treated KSL cells and progeny displayed a 40% reduction in percentage γ-H2ax, a marker for DNA breakage, compared with cultures with TSF alone (Fig. 4F). EGF may also facilitate dsDNA break repair through non-homologous end joining recombination via phosphorylation of DNA-protein kinase catalytic subunit (DNA-PKcs) [30]. Following 24 hours treatment with FdUMP and a 15-minute stimulation with EGF, C57Bl6 KSL cells display a 4.8-fold increase in phosphorylation of DNA-PKcs (T2637) compared with FdUMP treated cultures only (Fig. 4G, 4H). The increase in phosphorylation of DNA-PKcs corresponded to both a repression of PUMA and an increase in BCL-2 with EGF treatment (Fig. 4I). These data demonstrate that EGF could mediate both cell proliferation and survival by increasing phospho-DNA-PKcs and via partial inhibition of PUMA signaling.

EGF Induces G-CSF Receptor Expression Following 5-FU

G-CSF is the clinical standard for treatment of myelosuppression following chemotherapy [1, 3]. We sought to determine whether dual therapy of G-CSF and EGF would be synergistic for hematopoietic regeneration compared with monotherapy with either EGF or G-CSF alone. On day 4 following 5-FU and G-CSF + EGF, C57Bl6 mice display increased marrow cellularity compared with G-CSF-treated mice (Fig. 5A). Dual therapy resulted in both increased percentage and total $SLAM^+$KSL compared with either G-CSF or EGF monotherapy (Fig. 5B). The levels of $SLAM^+$KSL cells in mice treated with G-CSF + EGF were 4.2-fold greater than in mice treated with either G-CSF or EGF monotherapy. This increase in $SLAM^+$KSL corresponded to an increase in CFC content in mice treated with dual G-CSF + EGF compared with mice treated with monotherapy (Fig. 5C). Based on LTC-IC analysis, G-CSF + EGF increased HSC content by 3.3-fold compared with either G-CSF or EGF alone (Fig. 5D). These data suggest that dual therapy with G-CSF + EGF is synergistic to accelerate HSC regeneration. With either G-CSF or EGF, comparable levels of hematopoietic content were measured, which indicates that EGF could equally accelerate hematopoietic regeneration at the same levels as the current clinical standard G-CSF.

Since G-CSF and EGF can promote hematopoietic regeneration, we sought to determine whether G-CSF could modulate expression of EGFR, and conversely, whether EGF could modulate expression of G-CSF receptor (G-CSFR). This hypothesis is supported by reports that EGFR+ carcinomas could induce extreme leukocytosis, suggesting that EGF and hematopoietic growth factors other than exogenous G-CSF could promote leukocytosis via G-CSFR signaling [31, 32]. The gene that encodes G-CSFR *Csf3r* is increased 3.6-fold in KSL cells treated with chemotherapy and EGF compared with cultures with chemotherapy alone (Fig. 5E). To model this study in vivo, we administered 5-FU to C57Bl6 mice and then administered EGF

Figure 4. Epidermal growth factor (EGF) promotes cell cycling and decreases apoptotic cell death. **(A):** On day 4 following 5-fluorouracil (5-FU) and either EGF or saline, shown are representative flow cytometric analysis and quantification of Ki67+ C57Bl6 ckit + Sca + Lin- (KSL) cells. $n = 5$ per group. *, $p = .04$ by one-tailed Mann-Whitney analysis. **(B):** % KSL cells in G1 (white) or S + G_2M (gray). *, $p = .03$ by Mann-Whitney analysis. **(C):** Reverse transcriptase polymerase chain reaction (RTPCR) analysis of CDK1, CDK2, CDK4, and CDK6 in C57Bl6 bone marrow (BM) lin^- cells at 4 hours following culture with 0.5 μM 5-fluoro-2′-deoxyuridine 5′-monophosphate (FdUMP) + 20 ng/ml EGF (EGF) or FdUMP alone (TSF). RTPCR analysis of p21 at 24 hours. $n = 4$ per group. *, $p < .0002$. **(D):** % Annexin + 7AAD– cells (black) and % annexin + 7AAD+ cells (white) in KSL cells. $n = 6$–8 per group. *, $p = .005$ and *, $p = .002$ for TSF versus TSF + FdUMP and TSF + FdUMP versus TSF + FdUMP + EGF, respectively. **(E):** Representative flow cytometric analysis of % annexin + 7-AAD– cells (black bar) and % annexin + 7AAD+ cells (white bar) at day 4 after 5-FU. $n = 9$–10 mice per group. *, $p = .002$ and $< .0001$ for % annexin + 7AAD– cells and % annexin + 7-AAD+ cells, respectively. **(F):** Representative flow cytometric analysis of % γ-H2ax of KSL cells at 24 hours with FdUMP (dark gray) or FdUMP + EGF (blue). Isotype is shown in light gray. $n = 4$–5 per group. *, $p < .0001$. **(G):** BM lin^- cells stained with phospho-DNA-protein kinase catalytic subunit (PKcs) (T2637, green) at 24 hours with .5 μM FdUMP and 15 minutes with 20 ng/ml EGF or TSF. Scale bar = 20 μm. Quantification of percentage positive pixels for phospho-DNA-PKcs by surface area. $n = 3$–5 per group. *, $p = .02$. **(H):** Representative flow cytometric analysis and % phospho-DNA-PKcs (T2647) from BM lin^- cells treated for 24 hours with 0.5 μM FdUMP and 15 minutes with 20 ng/ml EGF or TSF. $n = 6$–8 per group. *, $p = .04$. **(I):** RTPCR analysis of PUMA and BCL-2 in C57Bl6 BM lin^- cells at 24 hours following culture with 0.5 μM FdUMP + 20 ng/ml EGF (EGF) or FdUMP alone (TSF). $n = 4$ per group. *, $p = .004$ and .0001 for PUMA and BCL-2, respectively. Abbreviations: EGF, epidermal growth factor; FdUMP, 5-fluoro-2′-deoxyuridine 5′-monophosphate; SSC, side scatter; TSF, thrombopoietin, stem cell factor, and FMS-like tyrosine kinase 3 ligand.

or saline and included an untreated control group (Fig. 5E). Similar to EGFR, 24 hours following treatment with 5-FU induces *Csf3r* expression (Fig. 5E). The addition of EGF administration further increases *Csf3r* expression by 3.6-fold compared with 5-FU treatment alone (Fig. 5E). Corresponding to *Csf3r* mRNA expression, we measured the expression of G-CSFR protein and found that G-CSFR is increased 1.8-fold with 5-FU treatment compared with untreated controls (Fig. 5F). Similarly, treatment with 5-FU and EGF increased G-CSFR by 18.5% compared with 5-FU alone (Fig. 5F). These results indicate that EGF induces both mRNA and protein expression of G-CSFR following 5-FU.

Following chemotherapy and G-CSF, EGFR expression within KSL cells increased by 50% in vitro and by 45% in vivo compared with controls (Fig. 5G, 5H). To determine whether this increased EGFR expression corresponded to increased

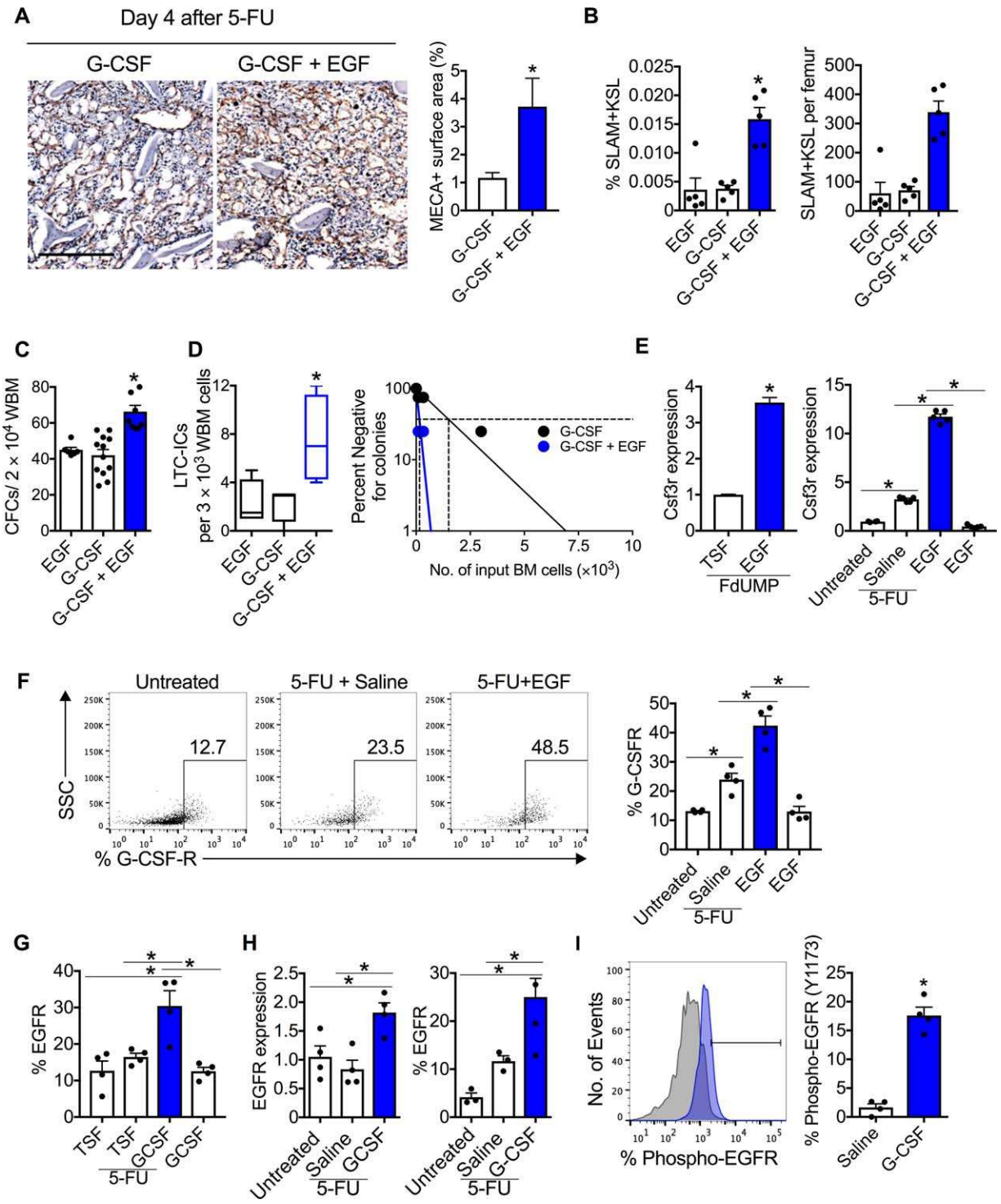

Figure 5.

EGFR signaling, the combination of 5-FU and G-CSF induced phosphorylation of EGFR (Y1173) compared with control mice (Fig.5I). These data demonstrate that EGF upregulates G-CSFR at both the levels of mRNA and protein expression. Complementary to this finding, G-CSF upregulates EGFR expression following chemotherapy and promotes phosphorylation of the EGF receptor.

EGFR Expression in Humans Is Induced Following 5-FU and G-CSF In Vivo

To make these findings translationally relevant and validate the findings from our murine studies, we sought to determine whether EGF could promote cancer growth in cancer cell lines. We used two cancer lines that were generated from patients with colorectal liver metastasis (CRC119 and CRC240) [21] and three lines purchased from ATCC (HT-29, HCT-116, and NCI-H460). Following culture with 20 ng/ml EGF for 72 hours, HCT-116 displayed a modest increase in cell viability compared with control cultures in media alone (Supporting Information Fig. S3A). All four other cell lines demonstrated no differences in cell expansion. Chemotherapy increased EGFR expression in CRC119 and in NCI-H460 and had no effect on other cell lines (Supporting Information Fig. S3B–S3D). These data indicate that a subset of tumors does not respond to EGF treatment and that chemotherapy does not increase EGFR expression in all cancer cell lines at the time points and concentrations tested.

Next, we examined whether 5-FU and G-CSF could modulate EGFR expression in vivo in humans. When patients with CRC were treated with 5-FU, the percentage of $CD34^+EGFR^+$ cells was 4.4-fold greater compared with untreated cancer patients and was higher than in healthy human donors (Fig. 6A). Following G-CSF injections, CD34+ PB from healthy human donors displayed a 4.3-fold increase in EGFR compared with CD34+ PB from untreated healthy human donors (Fig. 6B). This corresponded to a modest increase in phosphorylation of EGFR (Y1078) in G-CSF-treated donors (Fig. 6C). These data demonstrate that EGFR is both expressed and induced in vivo following treatment with either G-CSF or 5-FU.

Discussion

We have previously demonstrated that EGF is a hematopoietic growth factor using a cytokine screen from murine marrow supernatants [33]. Next, we have shown previously that following ionizing radiation injury, EGF could promote HSC regeneration [18]. Although EGF regulates HSC regeneration following radiation, whether EGF also regulates HSC regeneration following chemotherapy was unknown. This distinction is clinically relevant since the mechanisms driving hematopoietic regeneration may not be directly transposable between radiation and chemotherapy. Since there are key differences in the response of both hematopoietic cells and sinusoidal ECs to myelosuppressive injury from radiation and chemotherapy, we sought to address these differences in these current studies.

We demonstrate that EGF accelerates HSC regeneration following 5-FU. While a single injection of 5-FU may not impair the repopulating capacity of HSCs [34], 5-FU can both enrich the stem cell pool and induce functional changes on the enriched HSPC population [35]. 5-FU increased preferentially the expression of EGFR in HSPCs compared with more differentiated WBM cell populations. This expression of EGFR could prime both stem cells and stem/progenitor cells for EGF signaling to maximize the hematopoietic response when EGF is administered 24 hours later. Another mechanism by which EGF increased HSPCs is by increasing EC density in the marrow as measured by MECA+ vessels, thereby encouraging increased secretion of EGF. Using a pharmacologic approach by either supplementing EGF in cultures or EGF in vivo, we showed that increased levels of EGF resulted in increased HSC

Figure 5. Epidermal growth factor (EGF) and granulocyte colony stimulating factor (G-CSF) are synergistic for hematopoietic regeneration. **(A):** Left, mouse endothelial cell antigen-32 (MECA)- and hematoxylin-stained femurs from C57Bl6 mice treated with 5-fluorouracil (5-FU) on day 0 and G-CSF + EGF (days 1–4) or G-CSF alone (days 1–4). Scale bar = 250 μm. Right, quantification of percentage MECA+ pixels. $n = 5$ per group. *, $p = .04$ **(B):** Percentage $SLAM^+$ ckit + Sca + Lin- (KSL) cells and total $SLAM^+$KSL cells per femur at day 4 after 5-FU and treatment with EGF, G-CSF, or G-CSF + EGF on days 1–4. $n = 5$ per group. *, $p = .003$ and .004 for G-CSF + EGF versus EGF and versus G-CSF, respectively, for % $SLAM^+$KSL. *, $p = .0008$ and .0002 for G-CSF + EGF versus EGF and versus G-CSF, respectively, for $SLAM^+$KSL per femur. **(C):** Colony forming cell (CFC) content at day 4. $n = 6$–12 per group for CFCs. *$p = .000$ and $<.0001$ for G-CSF + EGF versus EGF and versus G-CSF, respectively. **(D):** Long-term culture initiating cells (LTC-ICs) on day 4 following 5-FU and G-CSF or G-CSF + EGF. $n = 4$ per group. *, $p = .04$. Poisson statistical analysis of a limiting dilution assay of 6-week LTC-ICs from bone marrow (BM) cells of C57Bl6 mice treated with G-CSF or G-CSF + EGF following 5-FU on day 4. The LTC-IC frequency of G-CSF + EGF-treated mice was 1 in 149 compared with 1 in 1,502 cells for G-CSF-treated mice ($n = 4$ per group per cell dose). **(E):** Left, *Csf3r* mRNA expression in KSL cells treated at 24 hours with 5-fluoro-2′-deoxyuridine 5′-monophosphate (FdUMP) and 20 ng/ml EGF or FdUMP alone. $n = 3$ per group. *, $p < .0001$. Right, *Csf3r* mRNA expression in whole bone marrow from C57Bl6 mice at 48 hours after 5-FU and 24 hours after EGF or saline compared with mice treated with EGF. Data were analyzed relative to Csf3r expression in untreated mice. $n = 4$–5 per group. *, $p < .0001$ for 5-FU + EGF versus saline, EGF (no 5-FU), or untreated mice. **(F):** Representative flow cytometric analysis and quantification of percentage G-CSF-R in KSL cells at 48 hours following 5-FU and 24 hours following EGF or Saline treatment in C57Bl6 mice. $n = 4$ per group. *, $p = .003$, .0002, and .0001 for 5-FU + EGF versus saline, EGF (no 5-FU), or untreated mice, respectively. **(G):** Percentage EGF receptor (EGFR) in KSL cells following 24 hours culture of BM lin^- cells with .5 μM FdUMP and 20 ng/ml G-CSF compared with FdUMP, G-CSF (no FdUMP), or untreated cells. $n = 4$ per group. *, $p = .02$, .006, and .01 for FdUMP + G-CSF versus FdUMP, G-CSF, and TSF only, respectively. **(H):** Left, EGFR mRNA expression after 1 hours 5-FU and G-CSF or saline for 10 minutes. $n = 4$ per group. *, $p = .005$ and .02 for 5-FU + G-CSF compared with 5-FU + saline and untreated control, respectively. Right, percentage EGFR in KSL cells at 48 hours following 5-FU and 24 hours following G-CSF or saline. $n = 3$–5 per group. *, $p = .04$ and .007 for 5-FU + G-CSF versus 5-FU + saline or untreated, respectively. **(I):** Representative flow cytometric analysis of percentage phosphorylation of EGFR (Y1173) in KSL cells at 10 minutes following 0.25 mg/kg body weight of G-CSF (blue) or saline (gray). Positive gating is noted by horizontal bar. $n = 4$ per group. *, $p < .0001$. Abbreviations: CFC, colony forming cell; EGF, epidermal growth factor; EGFR, epidermal growth factor receptor; 5-FU, 5-fluorouracil; G-CSF, granulocyte colony stimulating factor; G-CSFR, granulocyte colony stimulating factor receptor; KSL, ckit + Sca + Lin-; LTC-IC, long-term culture initiating cell; MECA, mouse endothelial cell antigen-32; TSF, thrombopoietin, stem cell factor, and FMS-like tyrosine kinase 3 ligand; WBM, whole bone marrow.

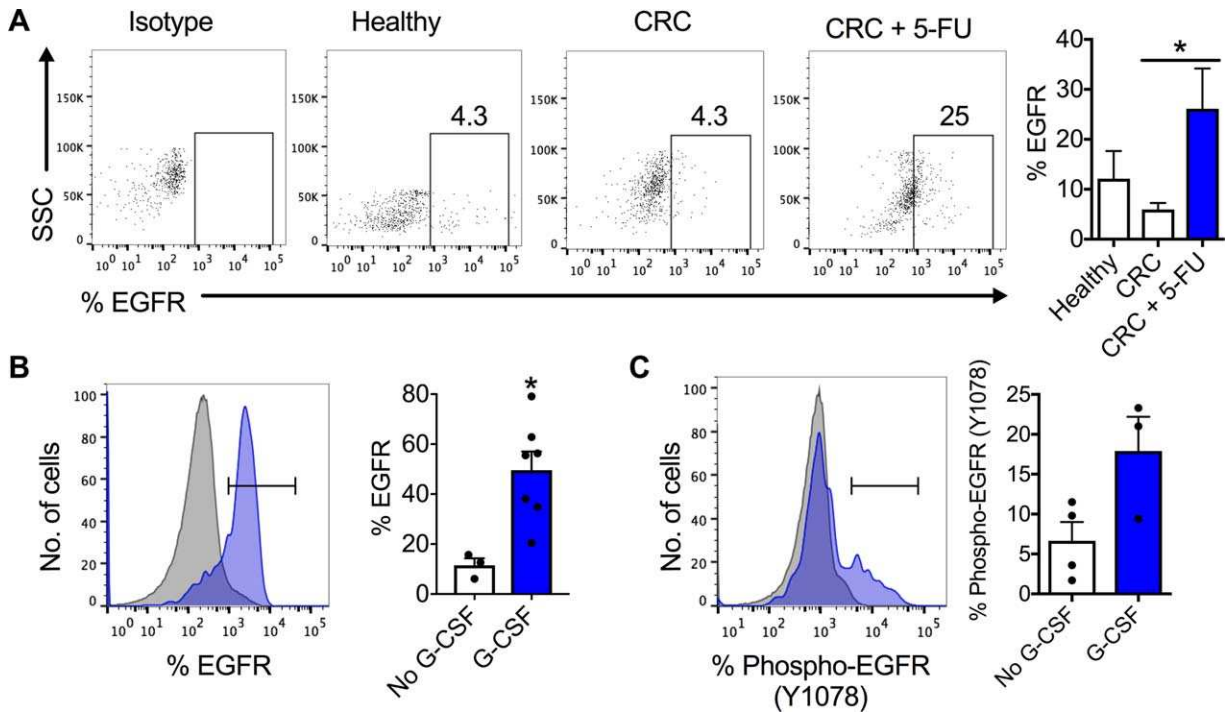

Figure 6. Epidermal growth factor receptor (EGFR) expression in humans is induced following 5-fluorouracil (5-FU) and granulocyte colony stimulating factor (G-CSF) in vivo. **(A):** Representative flow cytometric analysis and quantification of percentage EGFR in peripheral blood (PB) from patients with colorectal cancer (CRC) while on 5-FU treatment (CRC + 5-FU) compared with patients not on 5-FU treatment (CRC). Healthy human donor PB is shown for comparison. $n = 3–10$ per group. *, $p = .001$. **(B):** Percentage of EGFR+ cells and **(C)** phosphorylation of EGFR (Y1078) from CD34+ cells in the PB of healthy human donors at baseline and following G-CSF treatment. *, $p = .01$ for percentage EGFR, $n = 3–7$ per group. Abbreviations: CRC, colorectal cancer; EGFR, epidermal growth factor receptor; 5-FU, 5-fluorouracil; SSC, side scatter.

content after 5-FU. This increase in HSC content corresponded to an increase in myeloid progenitor engraftment, or a myeloid-bias following hematopoietic injury [18, 36].

Complementary to these pharmacologic gain-of-function studies, we used a genetic approach using *VECadherinCre;Bax*$^{FL/FL}$ (*Bax*$^{FL/FL}$) mice and littermate control mice. While baseline measurements of EGF were increased in *Bax*$^{FL/FL}$ ECs compared with *Bax*$^{FL/+}$ ECs, treatment with FdUMP further increased levels of EGF in both genotypes. These increased levels of EGF resulted in increased HSC content and accelerated hematopoietic regeneration after 5-FU. These results demonstrate that EGF is a hematopoietic growth factor that accelerates regeneration after myelosuppressive chemotherapy.

The mechanism by which EGF promotes cellular proliferation following chemotherapy is by upregulation of cyclin dependent kinases, in particular CDK1, CDK2, and CDK6. Upregulation of these CDKs permits cell cycle progression. For cells to enter S-phase, levels of the CDK inhibitor p21 should be low [27, 37]. In our system, EGF represses p21 expression following chemotherapy. In a report from Sheng et al. [38], EGF was shown to increase expression of p21 and promotes enterocyte proliferation. It is possible the effect of EGF on CDKs and CDK inhibitors is dose-dependent and could vary based on cell type (i.e., hematopoietic cells vs. enterocyte) and whether injury is present.

We demonstrate that dual therapy with G-CSF and EGF following 5-FU increased HSPC content within the marrow. When G-CSF and EGF are administered in combination following 5-FU, mice display increased HSPC compared with mice that received either agent alone, indicating the function of G-CSF has synergy with EGF. These findings are buffeted by a prior report that associated G-CSF and EGFR signaling [39]. Using a genetic approach, Ryan et al. localized the region that was responsible for G-CSF-mediated hematopoietic mobilization to a region within the EGFR locus [39]. Our data demonstrated increased hematopoietic stem/progenitor cell content in the marrow following 5-FU when G-CSF and EGF are co-administered. These data are consistent with published results showing that G-CSF and EGF treatment contributed to the retention of HSPCs in the marrow [39]. Without chemotherapy, EGF does not increase G-CSFR expression, and conversely, G-CSF does not alter EGFR expression. It is possible that this cross-induction of receptor expression requires an injured marrow, like that caused in the setting of chemotherapy. Finally, our results from murine models were validated in humans in which treatment with 5-FU increased levels of EGFR in CD34+ hematopoietic cells in vivo. Moreover, treatment with G-CSF in healthy human donors showed a modest increase in phosphorylation of EGFR within the CD34+ stem/progenitor cell pool.

Although EGF is a known mitogen, culture of cancer cell lines with EGF increased cell viability in only one of five cell lines. This cell line HCT-116 displayed high levels of EGFR expression. EGFR expression or mutational status is not assessed in patients with CRC, since its status does not predict response to anti-EGFR therapies [40]. Additional screens of cell lines are required to predict whether EGF could be administered without encouraging cancer cell proliferation.

The hematopoietic phenotype of mice with deficiency of EGFR or G-CSFR has been described previously [18, 41, 42]. Tissue-specific deletion of EGFR within cells of hematopoietic lineages resulted in no differences in complete blood counts nor ability to generate committed progenitors in methylcellulose assays in homeostasis [18]. Only following myelosuppressive radiation does the deficiency of EGFR delay hematopoietic stem/progenitor cell regeneration compared with animals with functional EGFR [18]. Mice that are deficient in G-CSFR have quantitatively decreased numbers of neutrophils, although these neutrophils have normal function and can emigrate appropriately to sites of inflammation [41]. Targeted deletion of the intracellular component of G-CSFR further impairs chemotaxis of neutrophils and neutrophil mobilization from the marrow following G-CSF administration [42]. These data demonstrate that G-CSFR is a major regulator of hematopoiesis in homeostasis, but whether EGFR and G-CSFR signaling are coordinated in response to myelosuppressive stressors are incompletely defined.

Clinical reports have suggested that EGF signaling might promote signal transduction through G-CSFR. Patient case studies suggest that a subset of lung carcinomas, of which about a 1/3 will bear EGFR-positive mutations [43], could produce cytokines that cause extreme leukocytosis or a leukemoid reaction [32], possibly by signal transduction through G-CSFR. For example, a patient with lung sarcomatoid carcinoma, that was highly positive for EGFR by immunohistochemistry, developed leukocytosis with 140×10^9 per liter WBC (normal range $3–10 \times 10^9$ per liter) in the absence of infectious symptoms and pharmacologic G-CSF treatment [32]. In a series of more than 550 patients with non-small cell lung cancers, 11% of patients presented with leukocytosis or thrombocytosis at the time of diagnosis [31]. This incidence of leukocytosis or thrombocytosis increases to 72% in patients with advanced-stage disease in non-small cell lung cancers and portends a poorer prognosis compared with patients without elevations in blood counts [31]. Other reports have suggested that EGFR-driven cancers could elaborate growth factors, including G-CSF and granulocyte-macrophage colony stimulating factor, to promote a cancer survival advantage [44]. Indeed, lung carcinoma in cultures supplemented with EGF had increased levels of G-CSF in the conditioned media compared with saline-treated cultures [45]. These data are suggestive that cancers with EGFR-positive mutations could promote leukocytosis. Whether leukocytosis was due to EGF and signal transduction through EGFR or G-CSFR remains to be defined. In addition, whether EGF preferentially binds to either EGFR or G-CSFR following 5-FU is still unknown.

Conclusion

EGF regulates HSC regeneration following myelosuppressive chemotherapy. When administered in combination with G-CSF, dual therapy results in synergistic activity. Translationally, EGF could be administered either as monotherapy or in combination with G-CSF to accelerate hematopoietic regeneration and improve the chances of cure for patients with EGFR-negative malignancies.

Acknowledgments

We thank David G. Kirsch, for providing *VEcadherinCre;Bax*$^{FL/+}$ and *Bax*$^{FL/FL}$ mice and Joel R. Ross, for preparation of the graphical abstract. This work was supported by National Cancer Institute of the National Institutes of Health (K08CA184552; to P.L.D.) and by Duke Cancer Institute as part of the P30 Cancer Center Support Grant (NIH CA014236; to P.L.D.).

Author Contributions

S.O.P. and A.Y.F.K.: collection and assembly of data, data analysis and interpretation, critical review of manuscript, final approval of manuscript; E.G.K.: collection and assembly of data, data analysis and interpretation; B.J.C. and N.J.C.: data interpretation, critical review of manuscript, final approval of manuscript; N.L.S. and J.P.C.: data interpretation, critical review of manuscript; D.S.H.: data interpretation, provision of study materials; P.L.D.: conception and design, financial support, collection and assembly of data, data analysis and interpretation, manuscript writing, final approval of manuscript

Disclosure of Potential Conflicts of Interest

The authors indicated no potential conflicts of interest.

References

1 Crawford J, Ozer H, Stoller R et al. Reduction by granulocyte colony-stimulating factor of fever and neutropenia induced by chemotherapy in patients with small-cell lung cancer. New Engl J Med 1991;325:164–170.

2 Kuderer NM, Dale DC, Crawford J et al. Impact of primary prophylaxis with granulocyte colony-stimulating factor on febrile neutropenia and mortality in adult cancer patients receiving chemotherapy: A systematic review. J Clin Oncol 2007;25:3158–3167.

3 Smith TJ, Bohlke K, Lyman GH et al. Recommendations for the use of wbc growth factors: American society of clinical oncology clinical practice guideline update. J Clin Oncol 2015;33:3199–3212.

4 Demetri GD, Griffin JD. Granulocyte colony-stimulating factor and its receptor. Blood 1991;78:2791–2808.

5 Kiel MJ, Yilmaz OH, Iwashita T et al. Slam family receptors distinguish hematopoietic stem and progenitor cells and reveal endothelial niches for stem cells. Cell 2005;121:1109–1121.

6 Mendez-Ferrer S, Michurina TV, Ferraro F et al. Mesenchymal and haematopoietic stem cells form a unique bone marrow niche. Nature 2010;466:829–834.

7 Chow A, Lucas D, Hidalgo A et al. Bone marrow cd169+ macrophages promote the retention of hematopoietic stem and progenitor cells in the mesenchymal stem cell niche. J Exp Med 2011;208:261–271.

8 Ding L, Saunders TL, Enikolopov G et al. Endothelial and perivascular cells maintain haematopoietic stem cells. Nature 2012;481:457–462.

9 Ding L, Morrison SJ. Haematopoietic stem cells and early lymphoid progenitors occupy distinct bone marrow niches. Nature 2013;495:231–235.

10 Himburg HA, Doan PL, Quarmyne M et al. Dickkopf-1 promotes hematopoietic regeneration via direct and niche-mediated mechanisms. Nat Med 2016;23:91–99.

11 Montfort MJ, Olivares CR, Mulcahy JM et al. Adult blood vessels restore host hematopoiesis following lethal irradiation. Exp Hematol 2002;30:950–956.

12 Chute JP, Muramoto GG, Salter AB et al. Transplantation of vascular endothelial cells mediates the hematopoietic recovery and

survival of lethally irradiated mice. Blood 2007;109:2365–2372.
13 Zachman DK, Leon RP, Das P et al. Endothelial cells mitigate DNA damage and promote the regeneration of hematopoietic stem cells after radiation injury. Stem Cell Res 2013;11:1013–1021.
14 Chute JP, Muramoto GG, Fung J et al. Soluble factors elaborated by human brain endothelial cells induce the concomitant expansion of purified human bm cd34+cd38- cells and scid-repopulating cells. Blood 2005; 105:576–583.
15 Himburg HA, Muramoto GG, Daher P et al. Pleiotrophin regulates the expansion and regeneration of hematopoietic stem cells. Nat Med 2010;16:475–482.
16 Chute JP, Saini AA, Chute DJ et al. Ex vivo culture with human brain endothelial cells increases the scid-repopulating capacity of adult human bone marrow. Blood 2002; 100:4433–4439.
17 Kobayashi H, Butler JM, O'donnell R et al. Angiocrine factors from akt-activated endothelial cells balance self-renewal and differentiation of haematopoietic stem cells. Nat Cell Biol 2010;12:1046–1056.
18 Doan PL, Himburg HA, Helms K et al. Epidermal growth factor regulates hematopoietic regeneration after radiation injury. Nat Med 2013;19:295–304.
19 Kojima E, Tsuboi A. Effects of 5-fluorouracil on hematopoietic stem cells in normal and irradiated mice. J Radiat Res 1992;33:218–226.
20 Hooper AT, Butler JM, Nolan DJ et al. Engraftment and reconstitution of hematopoiesis is dependent on vegfr2-mediated regeneration of sinusoidal endothelial cells. Cell Stem Cell 2009;4:263–274.
21 Lu M, Zessin AS, Glover W et al. Activation of the mtor pathway by oxaliplatin in the treatment of colorectal cancer liver metastasis. PloS One 2017;12:e0169439.
22 Stier S, Cheng T, Dombkowski D et al. Notch1 activation increases hematopoietic stem cell self-renewal in vivo and favors lymphoid over myeloid lineage outcome. Blood 2002;99:2369–2378.
23 Lehr HA, Mankoff DA, Corwin D et al. Application of photoshop-based image analysis to quantification of hormone receptor expression in breast cancer. J Histochem Cytochem 1997;45:1559–1565.
24 Ploemacher RE, van der Sluijs JP, van Beurden CA et al. Use of limiting-dilution type long-term marrow cultures in frequency analysis of marrow-repopulating and spleen colony-forming hematopoietic stem cells in the mouse. Blood 1991;78:2527–2533.
25 Calvi LM, Adams GB, Weibrecht KW et al. Osteoblastic cells regulate the haematopoietic stem cell niche. Nature 2003;425: 841–846.
26 Fabian MA, Biggs WH, 3rd, Treiber DK et al. A small molecule-kinase interaction map for clinical kinase inhibitors. Nat Biotechnol 2005;23:329–336.
27 Lim S, Kaldis P. Cdks, cyclins and ckis: Roles beyond cell cycle regulation. Development 2013;140:3079–3093.
28 Yoshioka A, Tanaka S, Hiraoka O et al. Deoxyribonucleoside triphosphate imbalance. 5-fluorodeoxyuridine-induced DNA double strand breaks in mouse fm3a cells and the mechanism of cell death. J Biol Chem 1987; 262:8235–8241.
29 Kriegs M, Kasten-Pisula U, Rieckmann T et al. The epidermal growth factor receptor modulates DNA double-strand break repair by regulating non-homologous end-joining. DNA Repair 2010;9:889–897.
30 Myllynen L, Rieckmann T, Dahm-Daphi J et al. In tumor cells regulation of DNA double strand break repair through egf receptor involves both nhej and hr and is independent of p53 and k-ras status. Radiother Oncol 2011;101:147–151.
31 Boddu P, Villlines D, Aklilu M. [paraneoplastic leukocytosis and thrombocytosis as prognostic biomarkers in non-small cell lung cancer]. Zhongguo Fei Ai Za Zhi 2016;19:725–730.
32 Wang D, Zhang H, Yu F et al. Extreme leukocytosis and leukemoid reaction associated with the lung sarcomatoid carcinoma: An unusual case report. Int J Gen Med 2016; Volume 10:7–9.
33 Doan PL, Russell JL, Himburg HA et al. Tie2(+) bone marrow endothelial cells regulate hematopoietic stem cell regeneration following radiation injury. Stem Cells (Dayton, Ohio) 2013;31:327–337.
34 Lerner C, Harrison DE. 5-fluorouracil spares hemopoietic stem cells responsible for long-term repopulation. Exp Hematol 1990; 18:114–118.
35 Randall TD, Weissman IL. Phenotypic and functional changes induced at the clonal level in hematopoietic stem cells after 5-fluorouracil treatment. Blood 1997;89:3596–3606.
36 Jiang C, Hu X, Wang L et al. Excessive proliferation and impaired function of primitive hematopoietic cells in bone marrow due to senescence post chemotherapy in a t cell acute lymphoblastic leukemia model. J Transl Med 2015;13:234.
37 Suryadinata R, Sadowski M, Sarcevic B. Control of cell cycle progression by phosphorylation of cyclin-dependent kinase (cdk) substrates. Biosci Rep 2010;30:243–255.
38 Sheng G, Bernabe KQ, Guo J et al. Epidermal growth factor receptor-mediated proliferation of enterocytes requires p21waf1/cip1 expression. Gastroenterology 2006;131: 153–164.
39 Ryan MA, Nattamai KJ, Xing E et al. Pharmacological inhibition of egfr signaling enhances g-csf-induced hematopoietic stem cell mobilization. Nat Med 2010;16:1141–1146.
40 Jonker DJ, O'callaghan CJ, Karapetis CS et al. Cetuximab for the treatment of colorectal cancer. New Engl J Med 2007;357: 2040–2048.
41 Liu F, Wu HY, Wesselschmidt R et al. Impaired production and increased apoptosis of neutrophils in granulocyte colony-stimulating factor receptor-deficient mice. Immunity 1996; 5:491–501.
42 Semerad CL, Poursine-Laurent J, Liu F et al. A role for g-csf receptor signaling in the regulation of hematopoietic cell function but not lineage commitment or differentiation. Immunity 1999;11:153–161.
43 Zhang YL, Yuan JQ, Wang KF et al. The prevalence of egfr mutation in patients with non-small cell lung cancer: A systematic review and meta-analysis. Oncotarget 2016;7: 78985–78993.
44 Akbay EA, Koyama S, Carretero J et al. Activation of the pd-1 pathway contributes to immune escape in egfr-driven lung tumors. Cancer Discov 2013;3:1355–1363.
45 Phan VT, Wu X, Cheng JH et al. Oncogenic ras pathway activation promotes resistance to anti-vegf therapy through g-csf-induced neutrophil recruitment. Proc Natl Acad Sci USA 2013;110:6079–6084.

See www.StemCells.com for supporting information available online.

